Controlling Technique of Induction Motor Drive using IGBT Chopper and Multi-Level Inverter for Enhanced Performance

Navneet kumar*[1], Abhishek Thakur*[2,] Geena Sharma*[3]
Navneet kumar- M.Tech Student, Abhishek Thakur- M.Tech Student, Geena Sharma- H.O.D./Assistant Professor Electrical Engg Deptt.
Navneet kumar*[1]- Electrical Engineering Deptt.
*BUEST Baddi University of Emerging Sciences and Technology Solan HP India

Abstract—Multilevel inverters continue to receive more and more attention because of their high voltage operation capability, low switching losses, high efficiency and low output of Electro Magnetic Interference (EMI). Induction motors are most commonly used motors in industrial applications, control systems as well as in main powered home appliances. Simple and rugged construction, low-cost, good efficiency, low maintenance, simplicity of control and direct connection to an ac power source are the main advantages of induction motors. Speed control of slip ring induction motor (SIM) has major role in controlled speed drive applications. The power semiconductor technology has played a crucial role in the advancement of variable speed induction motor drives employing slip power recovery scheme (SRS). SIM drive operates at limited speed range and has slip power a smaller part of motor power rating, hence low rating of converter and lower cost. This paper presents the performance characteristics of IGBT chopper and inverter-controlled SRS based IMD. The simulation model of IMD using IGBT based buck-boost chopper and pulse width modulated voltage source inverter (PWM) have been build up in MATLAB 2013b for performance evaluations. The performances of IMD have been investigated by taking in to account the parameters viz. power factor, efficiency and total harmonic distortion (THD). The simulation results signifies that the IGBT chopper and PWM voltage source inverter controlled SRS based IMD has higher power factor, efficiency with lesser THD in comparison of SRS with SCR inverter control.

Keywords— efficiency, power factor, slip power recovery scheme.

I. INTRODUCTION

A three phase induction motor is basically a constant speed motor so it is somewhat difficult to control its speed. The speed control of induction motor is done at the cost of decrease in efficiency and low power factor. Now a days, about 70% of industrial loads are run by induction motor drives. Induction motors are extensively used for smaller loads such as household appliances like fans, blowers, compressors and in the field where drive operation is intermittent i.e. hoists, cranes, conveyers, and lifts because the slip power can be easily controlled by slip rings. The slip power recovery scheme (SRS) controls the speed of SIM by sending back the feedback power to the supply mains thereby improves the efficiency of the SIM drive [1]. Slip ring induction motor drive works at limited speed range and has slip power a smaller part of motor power rating, hence low rating of converter and lower cost [2]. Because of advancement in the static converters technology, the researchers are drawing more interest in field of renewable energy sources [3-4]. The major demerit of slip power recovery scheme has been found to be as i) poor power factor of the supply, ii) requirement of higher reactive power and iii) high harmonic content [5-6]. Due to presence of harmonic contents there is a production of harmonic contents in the supply. In this literature survey, a number of methodologies [7] has been reported to enhance the performance of slip power recovery drive (SRD). A methodology employing buck chopper has operated the inverter at more secure firing angle and decrease consumption of reactive power. In this way, there is improvement in power factor and efficiency of Slip ring induction motor drive [8].

To control active and reactive power and also to decrease the harmonics content, various circuit configurations of PWM inverter and boost chopper have been utilized in the DC link of SRS in the rotor side [9, 10]. The utilization of buck-boost chopper has replaced one of the insulated gate bipolar transistor (IGBT) converters from the rotor circuit side by silicon controlled rectifier (SCR) converter and decrease the cost of SRS with the same performance parameters of induction machine [11]. Theoretically, the mathematical model has been shown to evaluate the DC link of SRD [12]. A twelve pulse SCR inverter with IGBT boost chopper has been modified to enhance the power factor, while SRD utilizing voltage source inverter (VSI) and boost chopper applying voltage controlled technique and current controlled technique reduces the total harmonic distortion (THD) of the source and also provides improved power factor [13-15]. A SRD system using buck converter and inverter with three PWM techniques in the intermediate circuit has been used with LC filter to decrease the harmonic contents of supply source [16]. The inverter configuration with step-down and step-up/step-down chopper has enhanced the power factor and efficiency of the SIM drives and quality of power supply [17, 18].

II. MATHEMATICAL MODELING OF SRS

Mathematical modeling of conventional SRS has been given in this subsection.

A. Model of the conventional SRS

In the diagram of slip power recovery scheme shown in "Fig.1", the three phase full-wave diode bridge rectifier connects to the windings of the rotor through slip rings. A part of slip power is converted in to DC by bridge rectifier and inverted into AC by a three-phase SCR inverter and feedback to the supply mains. The feedback power can be controlled by controlling the inverter voltage V_{d2}, by varying the firing angle of the inverter. The DC link inductor L_d has been provided to

reduce ripples in DC link current I_d and the transformer to match the voltages V_{d1} and V_{d2} by taking appropriate turn's ratio.

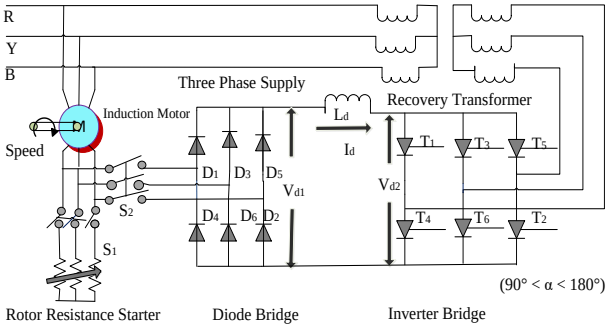

Fig. 1. Diagram of SRS utilizing SCR Inverter

Neglecting stator and rotor drops, the values of rectifier and inverter output voltages and slip can be described by equation (1)-(3) below [19].

$$V_{d1} = \frac{3\sqrt{2}}{\pi} \times \frac{sV}{n} \Rightarrow 1.35 \times \frac{sV}{n} \tag{1}$$

$$V_{d2} = \frac{3\sqrt{2}}{\pi} \times \frac{V}{m} \cos\alpha \Rightarrow 1.35 \times \frac{V}{m} \cos\alpha \tag{2}$$

$$s = \frac{n}{m} |\cos\alpha| \tag{3}$$

where V_{d1} and V_{d2} represents diode-bridge output voltages and inverter-bridge output voltages, α = the inverter firing angle, m = the turns ratio of transformer from source to converter side, n = the turns ratio of induction motor from stator to rotor side, s = the slip, V = the input voltage. Extreme value of α is enclosed to 165° for safe and secure commutation of thyristors. The desired and particular speed can be obtained with proper selection of firing angle [19].

The equations for DC link current, air-gap power, and electromagnetic torque are given by (3), (4), (5) and (10) below [18]

$$I_d = \frac{V_{d1} + V_{d2}}{2(sR_s^{'} + R_r) + R_d} \tag{4}$$

Neglecting copper loss

$$sP_g = |V_{d2}| I_d \Rightarrow 1.35 \times \frac{V}{m} \cos\alpha \times I_d \tag{5}$$

From equations (4) and (6)

$$P_g = 1.35 \frac{V}{n} \times I_d \tag{6}$$

$$P_m = (1-s) P_g = T_d \times \omega_r \tag{7}$$

$$\Rightarrow P_m = T_d \times \omega_m (1-s) \frac{2}{p} \tag{8}$$

The electromagnetic torque is given by

$$T_d = \frac{p}{2} \times \frac{P_g}{\omega_m} \tag{9}$$

From equations (7) and (10), electromagnetic torque can be expressed as

$$T_d = \left(\frac{p}{2}\right) \frac{1.35V}{n \times \omega_m} \times I_d \tag{10}$$

where, I_{dc} = DC link current, $R_s^{'}$ = rotor side referred stator resistance, R_r = rotor resistance, R_d = DC link inductor resistance, P_g = air gap power, T_d = electromagnetic torque, P_m = mechanical power at the shaft, ω_m and ω_r are the synch. speed and rotor speed in rad/sec, p = no of poles [20].

Equation (11) depicts that the torque is directly proportional to DC link current and the magnitude of which depends upon the voltage difference between the V_{d1} and V_{d2}. Consequently, the torque speed curves of IMD are approximately linear like separately excited DC motor for any particular value of inverter firing angle.

B. Proposed SRS Model with IGBT based Buck-Boost Chopper control technique

The demerit of the conventional SRS is high reactive power drawn from the source by the inverter when firing angle varies above 90°, which reduces power factor and quality of supply by increasing the THD. To overcome this problem, the proposed scheme has utilized the buck-boost chopper control technique as shown by "Fig.2", controlling the speed of the induction motor by duty ratio control at fixed value of α taking minimum reactive power from the source. Therefore, this technique will be able to reduce the reactive power consumption of the inverter thereby improves the power factor of the supply.

Taking in to consideration the DC link equivalent circuit of "Fig.2" the DC voltage of inverter, slip and DC link current can be written as [18]

$$V_{d2} = 1.35 \left(\frac{1}{1-\delta}\right) \frac{V}{m} \cos\alpha \tag{12}$$

$$\mathrm{s} = \frac{\mathrm{n}}{\mathrm{m}} \left(\frac{1}{1-\delta}\right) |cos\alpha| \tag{13}$$

$$I_d = \frac{V_{d1} - V_{d2}}{R_{dc}} \tag{14}$$

where, δ = duty ratio of chopper and R_{dc} = the DC link circuit is resistance which can be expressed as [13]

$$R_{dc} = \left\{2R_s' + \frac{3(X_s' + X_r)}{\pi}\right\} s + R_r + R_d \tag{15}$$

Air gap power, motor torque, and power factor are given by

$$sP_g = |V_{d2}| I_d \Rightarrow P_g = \frac{|V_{d2}| I_d}{s} \tag{16}$$

$$T = \frac{P_g}{\omega_m} \Rightarrow \frac{|V_{d2}| I_d}{s\omega_m} \tag{17}$$

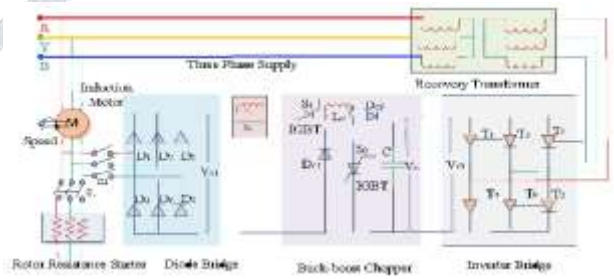

Fig. 2. Diagram of SRS employing SCR Inverter and buck-boost chopper

$$cos\phi = \frac{(P_s - P_r)}{\sqrt{(P_s - P_r)^2 + (Q_s + Q_r)^2}} \tag{18}$$

where X_s' = reactance of stator referred to rotor side and X_r = reactance of rotor respectively. P_s = active power and Q_s = reactive power consumed by inverter and motor from the supply source. P_r = active power recovered by inverter and Q_r = reactive power taken/recovered by the inverter from the supply source and is written as

$$P_r = 1.35V\left(\frac{1}{1-\delta}\right)cos\alpha \times I_d \quad (19)$$

$$Q_r = 1.35V\left(\frac{1}{1-\delta}\right)sin\alpha \times I_d \quad (20)$$

Equation (20) shows that the reactive power drawn from the source can be decreased by decreasing duty ratio keeping firing angle fixed which in turn increases the power factor as represented by equation (18). Hence the proposed scheme improves the power factor.

III. Modeling and Simulation of SRS

SRS employing the SCR inverter as shown in "Fig. 3," has been simulated in the MATLAB 2013b. The measurement blocks like Fourier block, and discrete block have been used to measure the speed, rms value of current, power factor of the current and the active and reactive power drawn from the source. The model of Induction motor drive having 2 hp, 415V, 50Hz, 1430 rpm has been simulated employing SCR inverter bridge. The model is running on MATLAB and different observations are plotted as shown in "Fig. 5,"-"Fig. 9," at various firing angle α of the inverter bridge. The efficiency and input-output powers can be given as in (22)-(25) below. The percentage efficiency of SIM can be expressed as

$$\eta_1 = \frac{P_{out}}{P_{in} - P_{fb}} \times 100 \quad (20)$$

The Fourier block has been connected to measure the speed, rms value of current and power factor of the current. Discrete block has been connected in the circuit to measure the active and reactive power. The proposed model used a 2 hp, 415V, 50Hz, 1430 rpm SRM for simulation and line commutated thyristors for the inverter bridge.

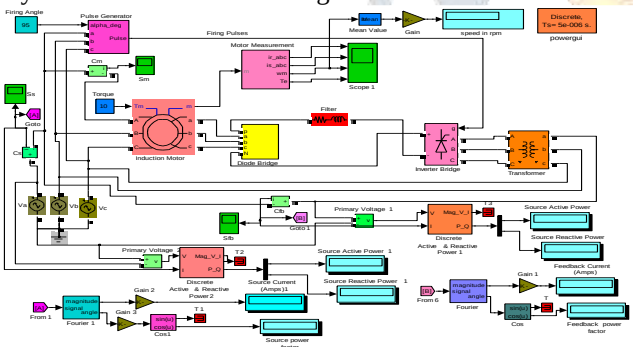

Fig. 3. Circuit Diagram of SRS Employing Natural Commutated SCR Inverter

By running the model on MATLAB and varying the firing angle of inverter the speed and other observations have been plotted as shown in "Fig. 5,"-"Fig. 9,". The efficiency, output powers, and rotor speed are given by (21) - (23) below [18]. The efficiency (%) of the motor is given by:

$$\eta_1 = \frac{P_{out}}{P_{in} - P_{fb}} \times 100 \quad (21)$$

where, η_1 = the %age efficiency of IMD, P_{in} = power input (W) and P_{fb} = power feedback (W) are the power measured by the measurement blocks and P_{out} = the mechanical power at the shaft (W) expressed as

$$P_{out} = \omega_r \times T_L \quad (22)$$

where ω_r is the rotor speed in rad/sec given as [20]

$$\omega_r = 2\pi \times \frac{N_r}{60} \quad (23)$$

where, T_L = load torque in Nm, N_r = rotor speed (rpm).

The proposed model of SRS shown in "Fig. 4," using IGBT chopper and inverter configuration is simulated in MATLAB. The speed of IMD is varied by varying duty-ratio of chopper (δ) from 80%-30% at an interval of 3% at fix value of inverter firing angle at 91°.The observed results of all the inverters configurations with IGBT buck-boost chopper have been plotted as shown in "Fig. 10," – "Fig. 14,".

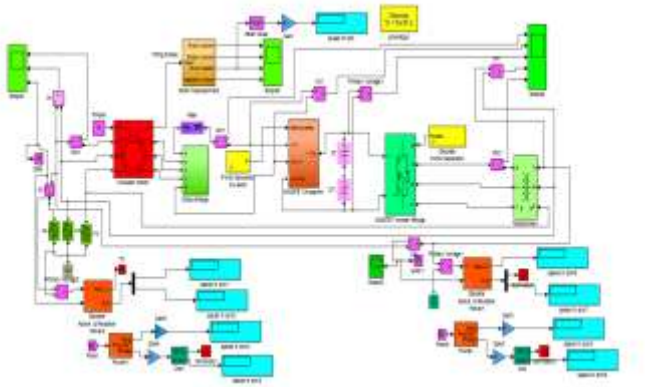

Fig. 4. Circuit Diagram of SRS Employing IGBT Based Buck-Boost Chopper and Inverter configuration

IV. Results and Disscussion

The following simulation results have been obtained on MATLAB for IMD. The results of "Fig. 5,"–"Fig. 9," show the curves of IMD using SRS with SCR inverter control technique.

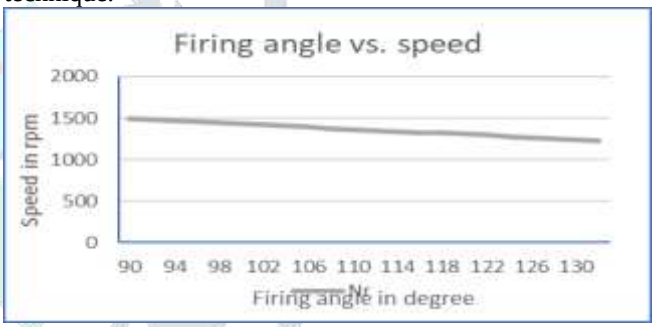

Fig. 5. Graph between firing angle and speed

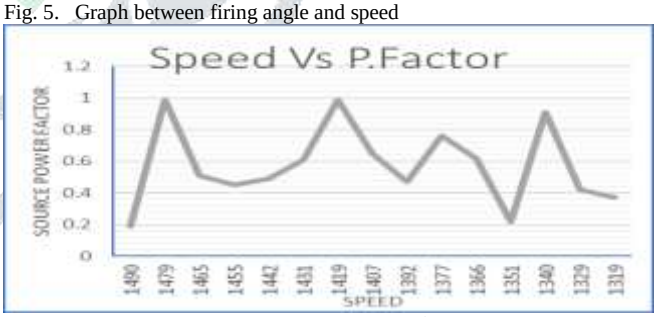

Fig. 6. Graph between speed and source power factor

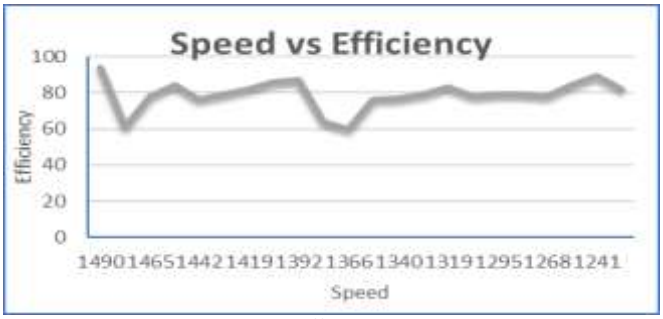

Fig. 7. Graph between speed and efficiency

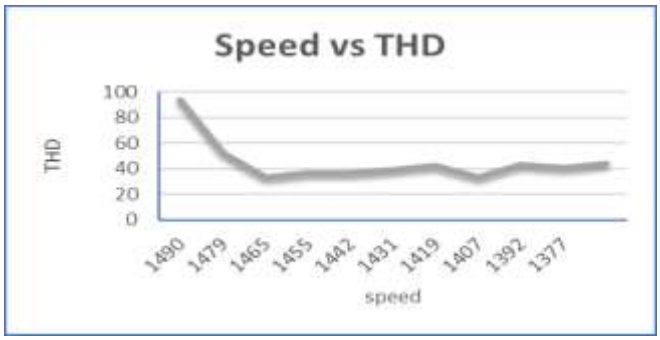

Fig. 8. Graph between speed and THD

A. Firing angle vs. speed

Simulation has been carried for one second and constant of 8 Nm was applied to the IMD. The variations of speed by varying the firing angle obtained from simulations have been shown in "Fig.5,". where the *Nr-1* indicates the rotor speed of induction motor with SCR inverter controller. The simulation results have shown that with the increase in firing angle of inverter the rotor speed decreases and vice versa.

B. Speed vs. source power factor

The graph of speed and source power factor has been shown in "Fig. 6," where the *cosφs-1* represents the source power factor. From the graph it is clear that there is decrease in source power factor with decrease in rotor speed. From the simulation results the average value of power factor is found to be 0.67.

C. Speed vs. efficiency

The graph of speed and efficiency has been shown in "Fig. 7," in which η-1 represent the efficiency of IMD. From the graph it is evident that with the decreases in rotor speed the efficiency of IMD also decreases. The average value of efficiency has been recorded as 86.5%. The increase in firing angle increases the feedback current which in turn increase the power loss in the feedback circuit hence slightly reduces the efficiency.

D. Speed vs. THD

"Fig. 8," shows the variations of the THD for different rotor speed where the *THD-1* indicating the THD of supply source. It has been observed from the graph that with the increase in firing angle or decrease in rotor speed, THD of the supply increases in case of inverter control. Because the increase in firing angle above 90° increases the reactive power consumption of inverter resulting in the increase in THD of the supply source.

E. Duty ratio vs. speed

The graph of duty ratio and rotor speed N_{r33} for IGBT chopper and inverter configurations has been shown in "Fig.9", From these curve it has been observed that with the increase in duty ratio of chopper, the rotor speed increases and vice versa.

F. Duty ratio vs. source power factor

The graph of duty ratio and source power factor for IGBT chopper and inverter configurations has been shown in "Fig. 10", From these curve it has been observed that with the increase in duty ratio of chopper, the source power factor improves.

The results of "Fig. 10," and "Fig. 11," show the curves of rotor speed and feedback power of IMD using SRS with IGBT chopper and PWM inverter control technique. The variations of source power factor, and THD w.r.t. speed have been shown in "Fig. 12,"–"Fig. 14,".

Fig. 9. Graph between duty ratio and speed

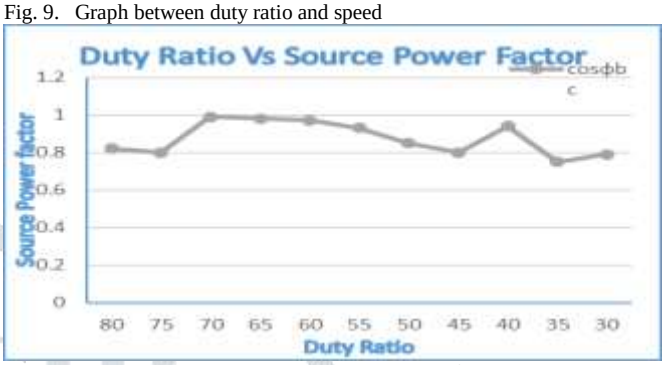

Fig. 10. Graph between duty ratio and source power factor

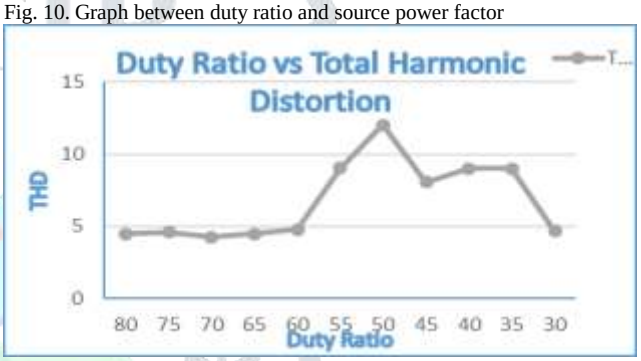

Fig. 11. Graph between duty ratio and total harmonic distortion

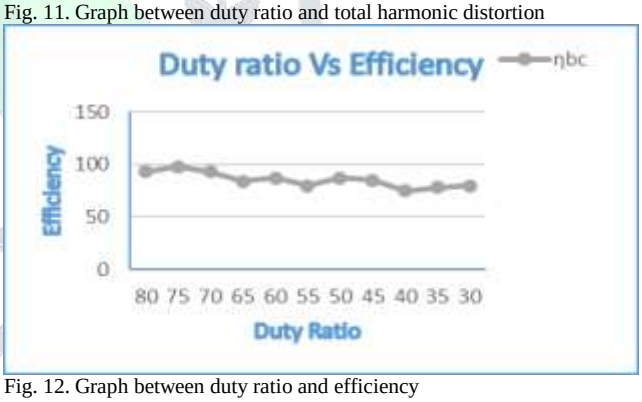

Fig. 12. Graph between duty ratio and efficiency

G. Duty ratio vs. total harmonic distortion

The graph of duty ratio and total harmonic distortion for IGBT chopper and inverter configurations has been shown in "Fig. 11", From these curve it has been observed that with the increase in duty ratio of chopper, distortion reduces.

H. Duty ratio vs. efficiency

The graph of duty ratio and efficiency for IGBT chopper and inverter configurations has been shown in "Fig. 12", From these curve it has been observed that with the increase in duty ratio of chopper, the efficiency improves.

The comparative curves of SRS with IGBT chopper and inverter configuration obtained from the simulations have been shown in "Fig.13"–"Fig.15". The results have been compared based on the equal speed range and load torque for

IMD.

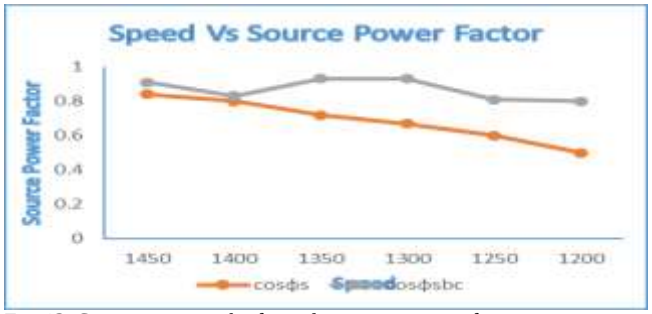

Fig. 13. Comparative graph of speed vs. source power factor

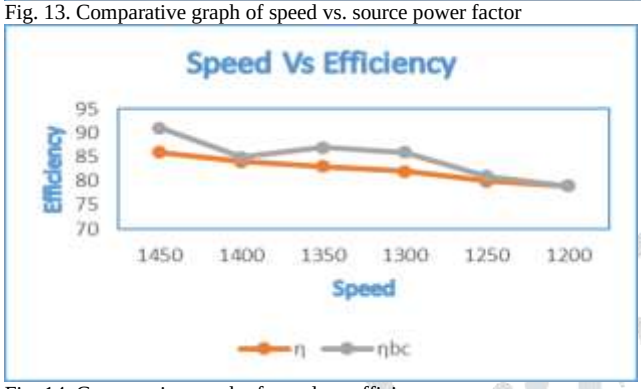

Fig. 14. Comparative graph of speed vs. efficiency

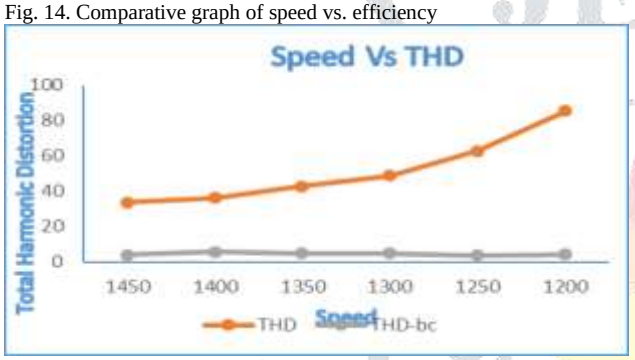

Fig. 15. Comparative graph of speed vs. THD

I. Speed vs. source power factor

"Fig. 13," shows the comparative graph of speed vs. source power factor employing SPRS with SCR inverter control and IGBT chopper control techniques having the average values of power factors viz. 0.67 and 0.9 respectively. The power factor decreases in both the cases decreases however the rate of decrement in the chopper control method is less therefore has higher power factor with a margin of 34.3% than that of inverter control.

J. Speed vs. efficiency

"Fig. 14," shows the comparative graph of speed and efficiency of IMD using SPRS with SCR inverter control and IGBT chopper control techniques having the average values of viz. 82 and 86.5 respectively. From the graph it is seen that the rate of decrease of efficiency has low in case of chopper control method. The chopper controller has higher average efficiency of 5.09% than inverter controller.

K. Speed vs. THD

"Fig. 15," shows the comparative graph of speed and efficiency of IMD using SPRS with SCR inverter control and IGBT chopper control techniques having the average values of i.e. 42.92 and 4.9 respectively. Hence chopper control technique has reduced the THD by a margin of 29.8% that from the inverter control.

V. Conclusions

The due study of IMD has been proposed in this paper employing IGBT chopper controlled SRS with IGBT chopper PWM voltage source inverter. The proposed IMD has been simulated in MATLAB 2013b employing SCR inverter control and IGBT chopper control with MOSFET inverter configuration. The power factor, efficiency and THD of source have been taken as parameters to examine the performance improvement of induction motor drive. From the above analysis and simulation results it has been observed that the IGBT chopper controller based SRS has improved the power factor of the source and less reactive is drawn from the source circuit. The efficiency of IMD is increased by a difference of 5.09% and THD of the supply source is reduced by a difference of 29.8% from the SCR inverter control method. These results have suggested the application of SRS using IGBT chopper and PWM voltage source inverter control method for better performance of IMD than SCR inverter control method. From all the above conclusions, by using boost chopper topology all the three characteristics i.e. power factor improves, efficiency gets higher and total harmonic distortion gets reduced.

References

[1] R. Ajabi-Farshba and M. R. Azizian, "Slip power recovery of induction machines using three-Level T -type converters," IEEE 5th Conference on Power Electronics, Drive Systems and Technologies, pp. 483-486, Feb 5-6, 2014.

[2] X. Yang, L. Xi, X. Yang, and Jian-guo Jiang, "Research on the application of PFC technology in cascade speed control system," IEEE 3rd Conference on Industrial Electronics and Applications ICIEA, pp. 1964-1969, 3-5 June, 2008.

[3] O. P. Rahi and A. K. Chandel, "Refurbishment and Uprating of Hydro Power Plants-A Literature Review," Renewable and Sustainable Energy Reviews, vol. 48, pp. 726-737, August 2015.

[4] O. P. Rahi and A. Kumar, "Economic Analysis for Refurbishment and Uprating of Hydro Power Plants," Renewable Energy, vol. 86, pp. 1197-1204, 2016.

[5] A. Lavi and R. J. Polge, "Induction motor speed control with static inverter in the rotor," IEEE Transaction on Power Apparatus and Systems, vol. PAS-85, pp. 76-84, 1966.

[6] W. Shepherd and J. Stanway, "Slip power recovery in an induction motor by the use of a thyristor inverter," IEEE Transactions on Industry and General Applications, vol. IGA-5, no. 1, pp. 74-82, 1969 .

[7] Sita Ram, O. P. Rahi, and Veena Sharma, "A comprehensive literature review on slip power recovery drives," Renewable and Sustainable Energy Reviews, vol. 73, pp. 922-934, 2017.

[8] P. Pilley and L. Refoufi, "Calculation of slip energy recovery induction motor drive behavior using the equivalent circuit," IEEE Transactions on Industry Applications, vol. 30, no. I. pp. 154-163, January/February 1994.

[9] G. D. Marques, "Numerical simulation method for the slip power recovery system," IEEE Proceedings of Electronic Power Application, vol. 146, no. 1, pp. 17-24, January 1999.

[10] G. D. Marques and P. Verdelho, "A simple slip-power recovery system with a dc voltage intermediate circuit and reduced harmonics on the mains," IEEE Transactions on Industry Electronics, vol. 47, no. 1, pp. 123-132, Feb. 2000.

[11] D. Panda, E. L. Benedict, G. Venkataramanan, and T. A. Lipo, "A novel control strategy for the rotor side control of a doubly-fed induction machine," IEEE Conference Record of 36th Annual meeting of Industry Applications, vol. 3, pp. 1695-1702, 30 September-4 October 2001.

[12] A. K. Mishra and A. K. Wahi, "Performance analysis and simulation of inverter fed slip -power recovery drive," IE (I) Journal-EL, vol. 85, pp. 89-95, Sept. 2004.

[13] S. Tunyasrirut, J. Ngamwiwita, V. Kinnares , T. Furuya, and Y. Yamamotod, "A DSP-based modified slip energy recovery drive using a 12-pulse converter and shunt chopper for a speed control system of a wound rotor induction motor," Electric Power Systems Research, vol. 78, no. 5, pp. 861–872, 2008.

[14] S. Tunyasrirut , V. Kinnares, and J. Ngamwiwit, "Performance improvement of slip energy recovery system by a voltage controlled technique," Renewable Energy, vol. 35, pp. 2235-2242, 2010.

[15] S. Tunyasrirut and V. Kinnares, "Speed and power control of a slip energy recovery drive using voltage-source PWM converter with current controlled technique," 10th Eco-Energy and Materials Science and Engineering Symposium, vol. 34, pp. 326-340, 2013.

[16] C. Pardhi, A. Yadavalli, S. Sharma, and G. A. Kumar, "A study of slip-power recovery schemes with a buck dc Voltage intermediate circuit and reduced harmonics on the mains by various PWM techniques," International

Conference on Computation of Power, Energy, Information and Communication, pp. 495-499, 2014.
[17] S. Ram, O. P. Rahi, V. Sharma, and A. Kumar, "Performance analysis of slip power recovery scheme employing two inverter topologies," Proceedings of MFIIS, vol. 2, pp. 356-361, 12-13 September 2015.
[18] Sita Ram, O. P. Rahi and Veena Sharma, " Analysis of induction motor drive using buck-boost controlled slip power recovery scheme," IEEE International Conference on Power Electronics, Intelligent Control and Energy Systems, pp. 1985-1990, 4-6 July, 2016 DTU.
[19] G. K Dubey, "Fundamentals of Electrical Drives," 1995, Narosa Public House Delhi.
[20] N. Mohan, T. M. Undeleand, and W. P. Robbin, "Power electronics converters, aplications, and design." Third Edition, Willey India Pvt. Ltd. New Delhi 2014.